Figures

Fig. 1

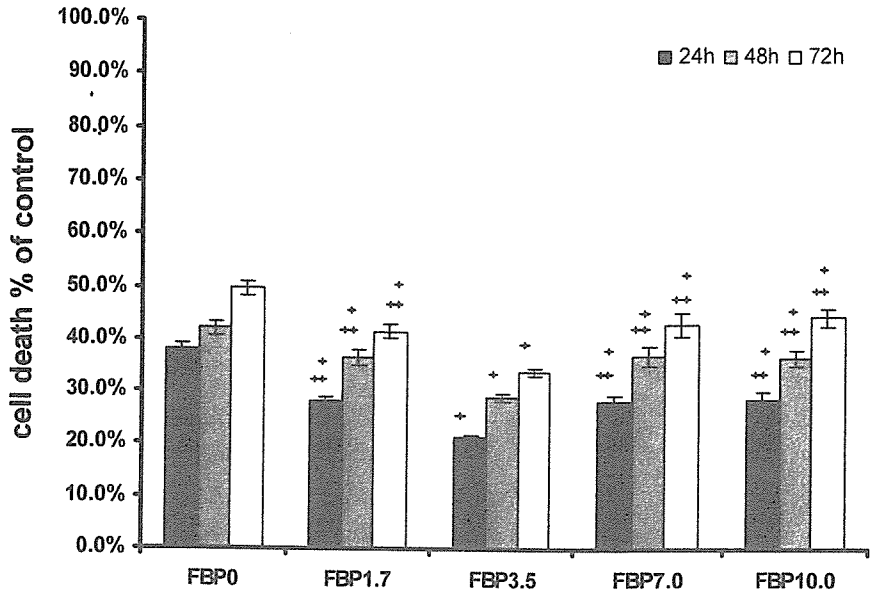

Fig. 2

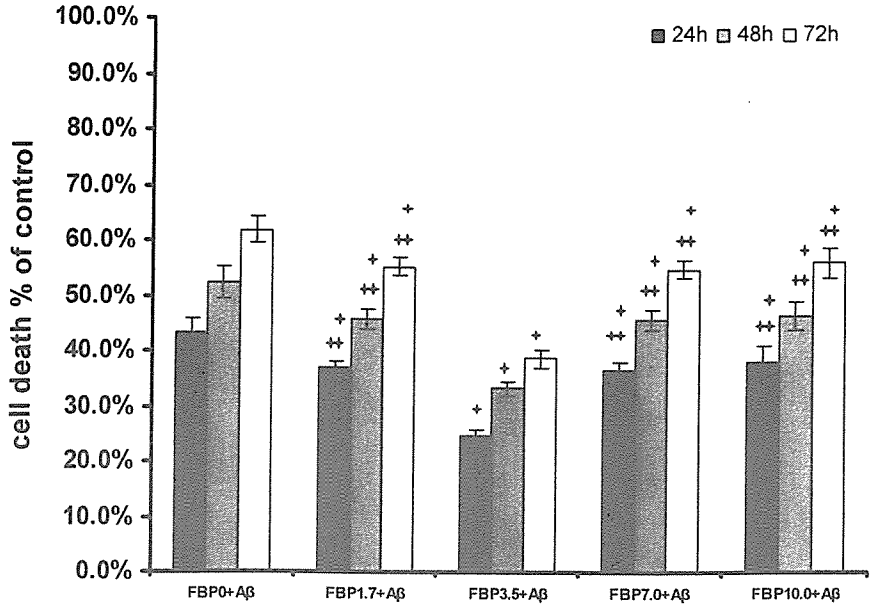
24h 48h 72h
cell death % of control
100.0%
90.0%
80.0%
70.0%
60.0%
50.0%
40.0%
30.0%
20.0%
10.0%
0.0%
FBP0+Aβ
FBP1.7+Aβ
FBP3.5+Aβ
FBP7.0+Aβ
FBP10.0+Aβ

Fig. 3

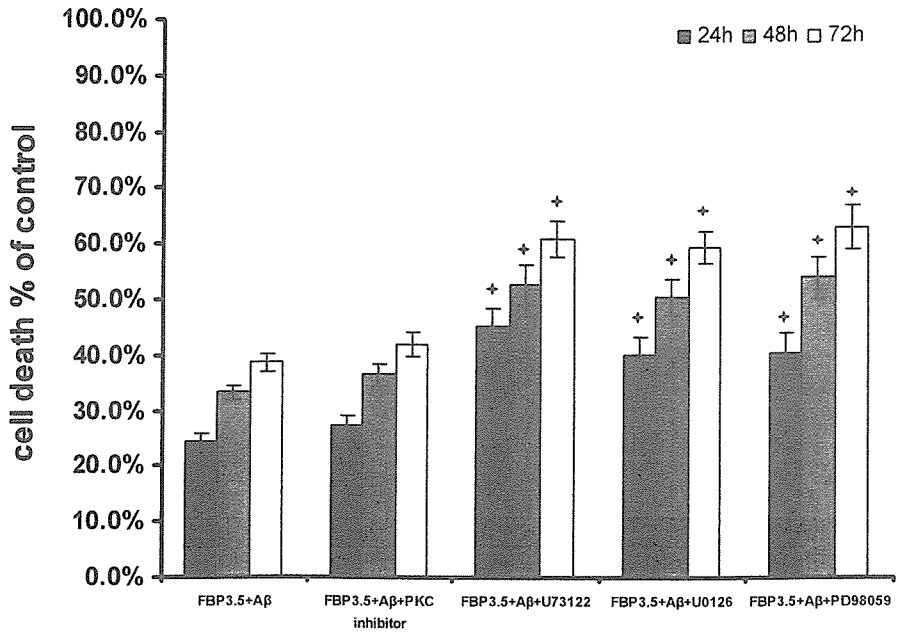
100.0%
90.0%
80.0%
70.0%
60.0%
50.0%
40.0%
30.0%
20.0%
10.0%
0.0%
cell death % of control
24h 48h 72h
FBP3.5+Aβ
FBP3.5+Aβ+PKC inhibitor
FBP3.5+Aβ+U73122
FBP3.5+Aβ+U0126
FBP3.5+Aβ+PD98059

Fig. 4

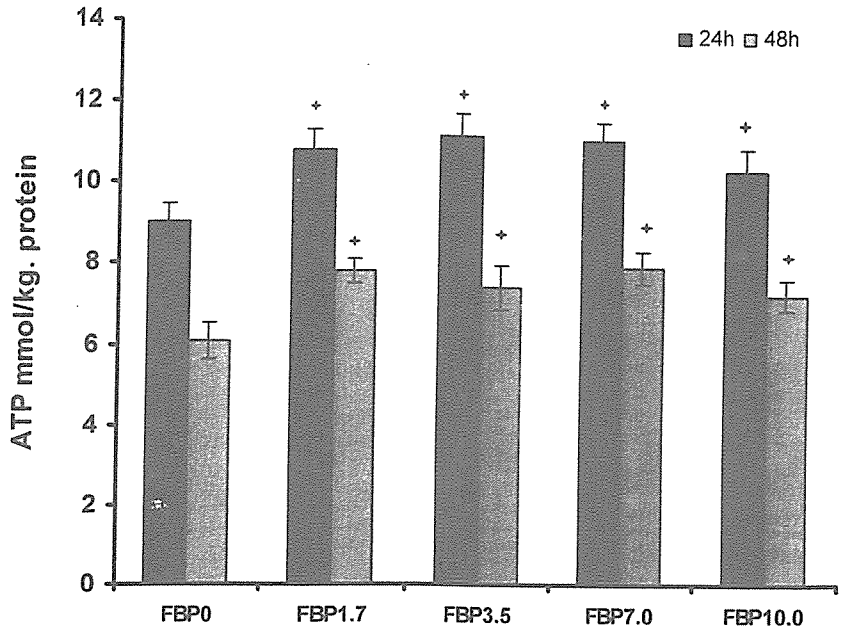
24h 48h
ATP mmol/kg. protein
14
12
10
8
6
4
2
0
FBP0
FBP1.7
FBP3.5
FBP7.0
FBP10.0

Fig. 5

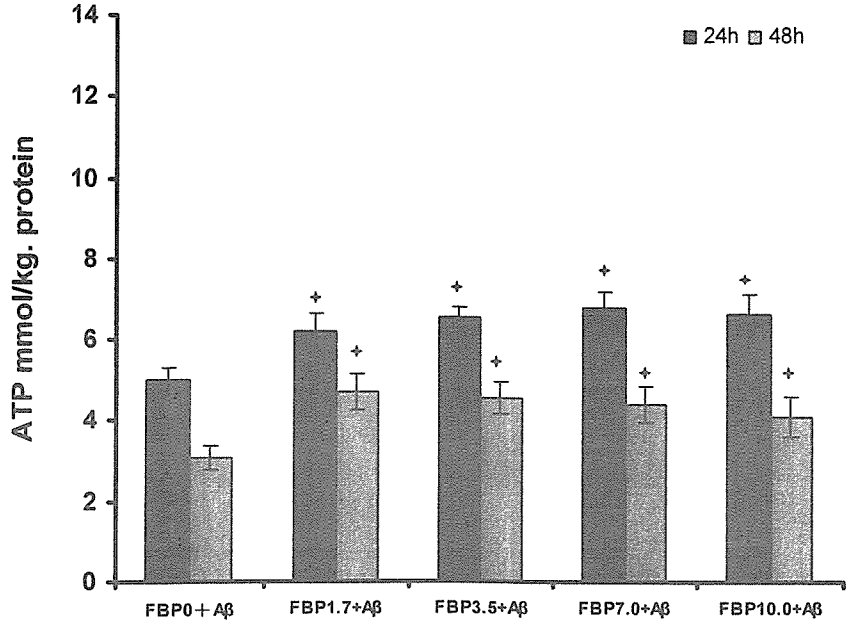
24h 48h
ATP mmol/kg. protein
14
12
10
8
6
4
2
0
FBP0+Aβ
FBP1.7+Aβ
FBP3.5+Aβ
FBP7.0+Aβ
FBP10.0+Aβ

Fig. 6

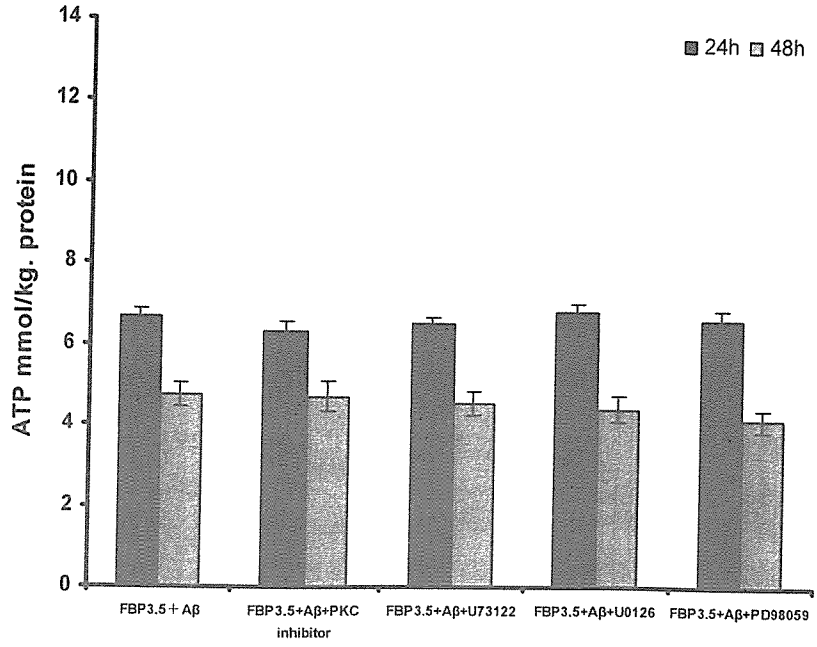
14
12
10
8
6
4
2
0
ATP mmol/kg. protein
24h
48h
FBP3.5+Aβ
FBP3.5+Aβ+PKC inhibitor
FBP3.5+Aβ+U73122
FBP3.5+Aβ+U0126
FBP3.5+Aβ+PD98059

Legends

Fig. 1. Neuroprotective effects of FBP on hippocampal organotypic slices culture. Various concentration of FBP were added to the media. Compared with control group (FBP 0 mM, n=36), the addition of FBP significantly reduced the cell death in hippocampal slices at 24h. 48h and 72h after treatment. FBP 3.5mM has better

Fig. 2. Neuroprotective effects of FBP against Aβ induced neurotoxicity on cultural hippocampal slices. Treatment with FBP significantly decreased Aβ induced cell death in hippocampal slices at 24h, 48h and 72h. FBP 3.5mM group has better

Fig. 3. Co-treatment with PLC inhibitor U73122 (n=45), MEK inhibitor U0126(n=39), and ERK inhibitor PD98059(n=48) attenuated the neuroprotective effect of FBP 3.5mM against Aβ induced neurotoxicity in hippocampal slices at 24h, 48h and 72h.

Fig. 4. Effects of FBP on the ATP levels of hippocampal slices in the absence of Aβ. Compared with control group (FBP 0 mM, n=48), FBP groups (concentration raging from 1.7 mM to 10 mM, each n=36) had significant elevated ATP levels in

Fig. 5. Effects of FBP on the ATP levels of hippocampal slices in the presence of Aβ. The ATP levels were preserved at each concentration of FBP. However, the difference of the ATP levels among these various FBP concentration groups(each n=36) did not reach to significance. *:compare with FBP 0 mM+Aβ group(n=36), all the $P<0.001$.

Fig. 6. Effects of PLC, MEK, ERK and PKC inhibitors on the ATP levels in hippocampal slices in the presence of FBP and Aβ. Co-treatment with PLC inhibitor(n=36), MEK inhibitor(n=36), ERK inhibitor or PKC inhibitor(n=36) did not cause significant difference in the ATP levels in hippocampal slices at 24h and 48h in the presence of FBP 3.5 mM and Aβ.

References

Alves,J.C., Santos, R.C., Castaman, T.A., Oliveira, J.R., 2004. Anti-inflammatory effects of fructose-1,6-bisphosphate on carrageenan-induced pleurisy in rat. Pharmacol Res. 49,245-248.

Bordignon, N.F., Meier, G.C., Alves, J.C., Lunardelli, A., Caberlon, E., Peres, A., Rodrigues, De., Oliveira, J., 2003.Immunomodulatory effect of fructose-1,6-bisphosphate on T-lymphocytes. Int. Immunopharmacol. 3,267-272.

Chlouverakis, C., 1968. The lipolytic action of fructose-1,6-diphosphate. Metabolism. 17,708–716.

Didlake, R., Kirchner, K.A., Lewin, J., Bower, J.D., Markov, A.K., 1989. Attenuation of ischemic renal injury with fructose 1,6-diphosphate. J Surg Res. Sep;47(3):220-6.

Donohoe, P.H., Fahlman, C.S., Bickler, P.E., Vexler, Z.S., Gregory, G.A., 2001.Neuroprotection and intracellular Ca^{2+} modulation with fructose-1,6-bisphosphate during in vitro hypoxia–ischemia involves phospholipase C-dependent signaling, Brain Res. 917,158–166.

Fahlman, C.S., Bickler, P.E., Sullivan, B., Gregory, G.A., 2002. Activation of the neuroprotective ERK signaling pathway by fructose-1,6-bisphosphate during hypoxia involves intracellular Ca^{2+} and phospholipase C. Brain Res. 958,43-51.

Fairas, L.A., Willis, M., Gregory, G.A., 1986. The effects of fructose 1-6 diphosphate glucose and saline on cardiac resuscitation. Anesthesiology. 65,595–601.

Galzigna, L., Rizzoli, V., Bianchi, M., Rigobello, M.P., Scuri, R., 1989. Some effects of fructose-1,6-diphosphate on rat myocardial tissue related to a membrane-stabilizing action. Cell Biochem Funct. 7,91-96.

Gobbel, G.T., Chan, T.Y., Gregory, G.A., Chan, P.H., 1994. Response of cerebral endothelial cells to hypoxia: modification by fructose-1,6-bisphosphate but not glutamate receptor antagonists. Brain Res. 653,23–30.

Gregory, G.A.,Yu, A.C.H., Chan,P.H., 1989. Fructose-1,6-bisphosphate protects astrocytes from hypoxia damage. J. Cereb. Blood. Flow Metab.9,29-34.

Gregory, G.A, Welsh, F.A., Yu, A.C., Chan, P.H., 1990. Fructose-1,6-bisphosphate reduces ATP loss from hypoxic astrocytes. Brain Res. 516,310-312.

Hardin, C.D., Roberts, T.M., 1994.Metabolism of exogenously applied fructose 1,6-bisphosphate in hypoxic vascular smooth muscle. Am. J. Physiol. 267,2325-2332.

Hassinen, I.E., Nuutinen, E.M., Ito, K., Nioka, S., Lazzarino, G., Giardina ,B.,Chance, B., 1991. Mechanisms of the effect of exogenous fructose 1,6-bisphosphate on myocardial energy metabolism. Circulation. 83,584–593.

Iwata, N., Higuchi, M., Saido, T,C., 2005.Metabolism of amyloid-beta peptide and Alzheimer's disease. Pharmacol.Ther. 18, Epub ahead of print.

Izumi, Y., Benz, A.M., Katsuki, H., Matsukawa, M., Clifford, D.B., Zorumski, C.F., 2003. Effects of fructose-1,6-bisphosphate on morphological and functional neuronal integrity in rat hippocampal slices during energy deprivation. Neuroscience.116,465-475.

Kelleher, J.A., Chan, P.H., Chan, T.Y., Gregory, G.A., 1995. Energy metabolism in

hypoxic astrocytes: protective mechanism of fructose-1,6-bisphosphate. Neurochem. Res. 20,785-792.

Larrabee MG., 1980. Metabolic disposition of glucose carbon by sensory ganglia of 15-day-old chicken embryos, with new dynamic models of carbohydrate metabolism. J Neurochem. Jul;35(1):210-31.

Lazzarino, G., Viola, A.R., Mulieri, L., Rotilio, G., Mavelli, I., 1987. Prevention by fructose-1,6-bisphosphate of cardiac oxidative damage induced in mice by subchronic doxorubicin treatment. Cancer Res. 47,6511-6516.

Liniger, R., Popovic, R., Sullivan, B., Gregory, G.A., Bickler, P.E., 2001. Effects of neuroprotective cocktails on hippocampal neuron death in an in vitro model of cerebral ischemia. J Neurosurg Anesthesiol. 13,19–25.

Markov, A.K., Oglethorpe. N., Grillis, M., Neely, W.A., Hellems, H.K,. 1983. Therapeutic action of fructose-1,6-diphosphate in traumatic shock. World J. Surg. 7,430–436.

Mattson, M.P., 1997. Cellular actions of beta-amyloid precursor protein and its soluble and fibrillogenic derivatives. Physiol. Rev.77, 1081 - 1132.

Musashi, M., Ota, S., Shiroshita, N., The role of protein kinase C isoforms in cell proliferation and apoptosis. Int. J. Hematol. 2000. 72,12-19.

Nunes, F.B., Graziottin, C.M., Alves, F.J.C., Lunardelli, A., Pires, M.G., Wachter, P.H., De, Oliveira, J.R., 2003. An assessment of fructose-1,6-bisphosphate as an antimicrobial and anti-inflammatory agent in sepsis. Pharmacol. Res. 47,35-41.

Okada, Y., 1974. Recovery of neuronal activity and high-energy compound level after complete and prolonged brain ischemia. Brain Res. 72, 346–349.

Rigobello,M,P., Bianchi,M., Deans,R.,Galzigna.,1982.Interaction of fructose-1,6-bisphosphate with some cell membranes. Agressologie.23,63-66.

Saito, N., Shirai, Y., 2002. Protein kinase C gamma (PKC gamma): function of neuron specific isotype. J. Biochem (Tokyo). 132,683-687.

Sakaguchi, T., Okada, M., Kawasaki, K., 1994.Sprouting of CA3 pyramidal neurons to the dentate gyrus in rat hippocampal organotypic cultures. Neurosci. Res. 20,157-164.

Sakurai,T.,Yang, B., Takata,T.,Yokono,K., 2002. Synaptic adaptation to repeated hypoglycemia depends on the utilization of monocarboxylates in Guinea pig hippocampal slices. Diabetes.51,430-438.

Sola, A., Berrios, M., Sheldon, R.A., Ferriero, D.M., Gregory, G.A., 1996. Fructose-1,6-bisphosphate after hypoxic ischemic injury is protective to the neonatal rat brain. Brain Res.741,294–299.

Takata, T., Nabetani, M., Okada, Y., 1997. Effects of hypothermia on the neuronal activity, [Ca^{2+}] accumulation and ATP levels during oxygen and/or glucose deprivation in hippocampal slices of guinea pigs. Neurosci. Lett. 227,41–44.

Tavazzi, B., Cerroni, L., Di, Pierro, D., Lazzarino, G., Nuutinen, M., Starnes, J.W., Giardina, B., 1990. Oxygen radical injury and loss of high-energy compounds in anoxic and reperfused rat heart: prevention by exogenous fructose-1,6-bisphosphate. Free Radic Res. Commun.10,167-176.

Yanagisawa K., 2000. Neuronal death in Alzheimer's disease. Int.Med.39,328-330.

Zhang, J.N., Zhang, F.M., Ma, W.S., Forrester, T., 1988. Protective effect of exogenous fructose-1,6-diphosphate in cardiogenic shock. Cardiovasc. Res. 22,927–932.

Zubairu, S., Hothersall, J.S., El-Hassan, A., McLean, P., Greenbaum, A.L., 1983. Alternative pathways of glucose utilization in brain: changes in the pattern of glucose utilization and of the response of the pentose phosphate pathway to 5-hydroxytryptamine during aging.J. Neurochem. 41,76-83.

TECHNICAL NOTE

Radiation Medicine: Vol. 22 No. 1, 56–59 p.p., 2004

Imaging of Fine Structure of Bone Sample with High Coherent X-ray Beam and High Spatial Resolution Detector

Masatsugu Hirano,[1] Katsuhito Yamasaki,[2] Riko Kitazawa,[3] Sohei Kitazawa,[3] Hiroshi Okada,[4] Tetsuro Katafuchi,[9] Takashi Sakurai,[5] Takeshi Kondoh,[6] Chiho Ohbayashi,[8] Sakan Maeda,[3] Kazuro Sugimura,[7] and Shinichi Tamura[1]

In this study, we observed bone specimens of the mouse using a very high coherence beam and high spatial resolution detector (zooming tube: approximately 0.7 micron resolution) and successfully obtained images of the Haversian canal, osteocytes, and osteoclasts.

Key words: X-ray imaging, synchrotron radiation, high spatial resolution, Haversian canal, osteocyte, osteoclast

Introduction

Although the technology of X-ray diagnostic equipment has improved markedly, conventional absorption imaging is limited in that its application to the observation of objects with small absorption rates is difficult. Expectations are mounting for the development and realization of a next-generation coherent X-ray source similar to that of the laser. Refraction contrast by X-rays (synchrotron radiation) of such high coherence would enable higher contrast imaging, which would reflect object density differently than the absorption imaging method.[1] Radiation dose can be reduced and spatial resolution can be improved using synchrotron radiation X-rays.[2,3] Thus, there is potential for clinical application to detect breast cancer.[4] Refraction contrast imaging by generating bright and dark lines on the object interface[5] has the effect of improving visibility.[3,6] Further, phase contrast CT has been developed by Momose *et al.*[7] It has been impossible to obtain such images with conventional radiation sources owing to their low degree of coherence. However, third-generation radiation sources have provided highly coherent imaging. Contrast imaging can be applied to the fields of orthopedics, breast cancer, and respiratory systems, among others. This success is due to the high spatial resolution detector and well-collimated X-ray beam.

Materials and Methods

This experiment was performed with a RIKEN Coherent X-ray Optics beam line (BL29XU at SPring-8). The schema of the set-up is shown in Fig. 1. The X-ray detector was zooming tube C5333 (Hamamatsu Photonics K.K., Shizuoka, Japan). The measured spatial resolution of the detector was 0.7 μm at 8 keV.[8] The X-ray energy was set at 12.4 keV by a monochromator in this experiment. The sample was placed at a distance of about 990 m downstream of the slit and 1.6 m upstream of the detector. The coherence length was approximately 200 μm. For example, the spatial coherence length of Photon Factory (PF BL-14C), a second-generation facility of synchrotron radiation, is 11 μm.[9]

Resected fibula of mouse (diameter, 300 μm) was used as a specimen to avoid overlapping of bone tissue and provide clear observation.

X-ray flux in front of the sample was measured at about 1.5×10^{11} photon/sec by ion-chamber, and beam exposure time was 20 sec. Therefore the radiation dose was estimated at about 18 Gy.

Received August 5, 2003; revision accepted November 1, 2003.

[1]Division of Interdisciplinary Image Analysis, Osaka University Graduate School of Medicine

[2]Japan Synchrotron Radiation Research Institute

Departments of [3]Pathology, [4]Urology, [5]Internal and Geriatric Medicine, [6]Neurosurgery, and [7]Radiology, Kobe University Graduate School of Medicine

[8]Department of Pathology, Kobe University Hospital

[9]National Cardiovascular Center

Reprint requests to Masatsugu Hirano, Interdisciplinary Image Analysis, Osaka University Graduate School of Medicine, D11, 2-2 Yamadaoka, Osaka 565-0871, JAPAN.

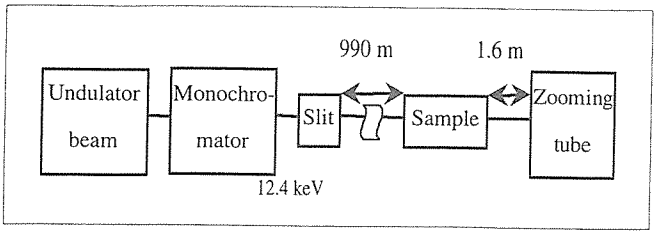

Fig. 1. Schema of set-up.

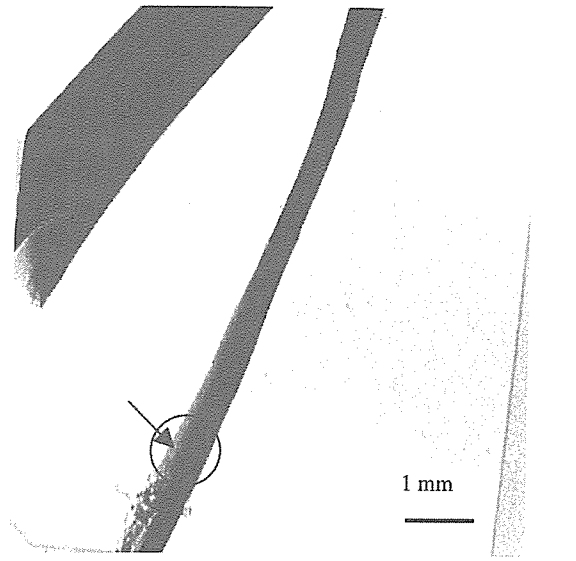

Fig. 2. Overview image of bone sample obtained with the bending magnet beamline.

Results

The reference image of the sample placed about 1 m downstream of the slit and about 2 m upstream of the 6 μm pixel size detector at the SPring-8 bending-magnet beamline is shown in Fig. 2. The same sample was imaged with high resolution at BL29XU (Fig. 3). Tube structure was observed in the center of the tissue. Measured diameter was 30-40 μm. This was assumed to be the Haversian canal. The cecal tube was connected to the Haversian canal. A cell-like structure with a multiangular margin observed at the end of the cecal tube was assumed to be an osteoclast. A fine tubular structure observed parallel to the Haversian canal was assumed to be a small blood vessel or canaliculus. The diameter of the fine tube was about 3 μm, and a spindle structure observed around it was assumed to be an osteocyte. These were 20-40 μm in size. The measured sizes of structures are compared with those of reference10 in Table 1. Sizes are smaller than those of the adult human because the sample was from a mouse fetus. These are the world's first radiographic images of fine structures of bone obtained using a high coherence X-ray beam with high spatial resolution.

Discussion

Using beamline BL20B2 at SPring-8, Mori *et al.* investigated bone samples with mammography film whose spatial resolution was a few microns.[9] Our imaging was done with a detector whose spatial resolution was 0.7 microns. The measured size of osteocytes and osteoclasts was more than 10 μm, and imaging was performed adequately.

This beam can be regarded as a parallel beam. The size of the field view in Fig. 3a is about 300 μm, almost equivalent to the coherence length. This means that the field view has very high coherence, and the coherence improves the contrast and produces high visibility owing to the refraction effect of X-rays at the object's boundary. A bright line was observed inside the Haversian canal and a dark line outside it. Such pairs of lines originated from the refraction of X-rays. Refraction occurred at the wall of the Haversian canal. The ray-tracing method simulated this refraction. The diameter of tube was 30 μm, and the densities in and outside the tube were assumed to be 1.0 and 1.7, respectively. Experimental and simulated images of the Haversian canal are shown in Fig. 5a and 5b, respectively. Profile curves of X-ray intensity are shown in Fig. 5c. The slope of the outside of the Haversian canal was smaller than the simulated slope. This means that density transition is low at the wall of the Haversian canal. Figure 6a shows a canaliculus, small blood vessel, osteocyte, and trabecula. These structures are periodic and parallel to the Haversian canal. Figure 6b shows a profile curve along the line in Fig. 6a. This curve shows periodic structure. Figure 6c shows the auto-correlation function of this profile curve. The auto-correlation function revealed the periodic pattern of these structures. Although speckles are sometimes observed using coherent X-ray imaging, our measurement showed no random speckles. However, it is possible that non-random pattern speckles are able to exist. There is no physical method to distinguish non-random speckles and the radiographic pattern of anatomical fine structure. The only method of distinguishing them is diagnostic observation by a radiologist.

Conclusion

In this study, fine structure of bone was successfully observed using high coherence X-rays. Contrast was improved incredibly using high coherence X-rays. Bone imaging can be performed using a light microscope or electron microscope, but many structures are destroyed

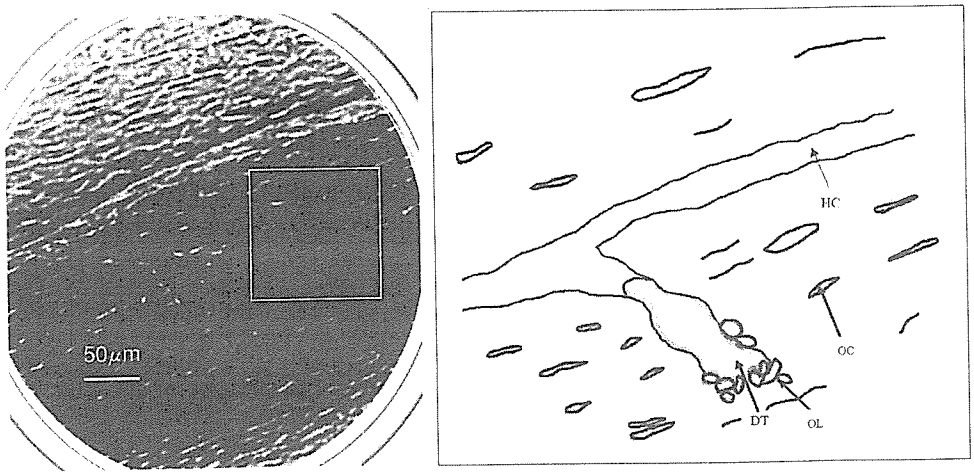

a | b

Fig. 3. a: Magnified image of Fig. 2 (circle) with coherent X-ray optics beam line.
b: Schema of Fig. 3a. Haversian canal (HC), osteocyte (OC), osteoclast (OL), and tunnel in bone tissue (DT) are shown.

Table 1. Diameters of the Haversian canal, osteocytes, and osteoclast measured in this experiment compared with those of adult human in reference 10

	Diameter of Haversian canal (μm)	Osteocytes (μm)	Osteoclasts (μm)
Experimental data	30-40	20-40	10-20
Data from reference	ca. 70	10-50	30-80

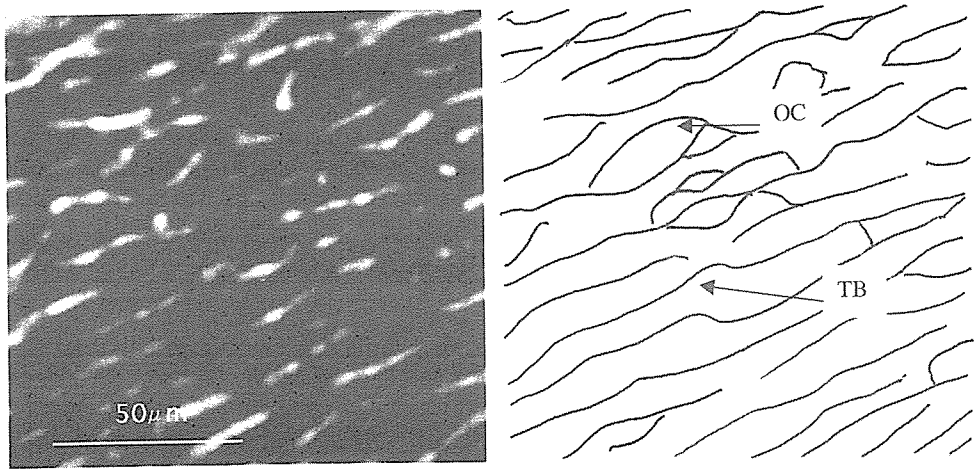

a | b

Fig. 4. a: Magnified image of Fig. 3 (rectangle). Trabecula is easily observed.
b: Schema of Fig. 4a. Osteocyte (OC) and trabecula (TB) are shown.

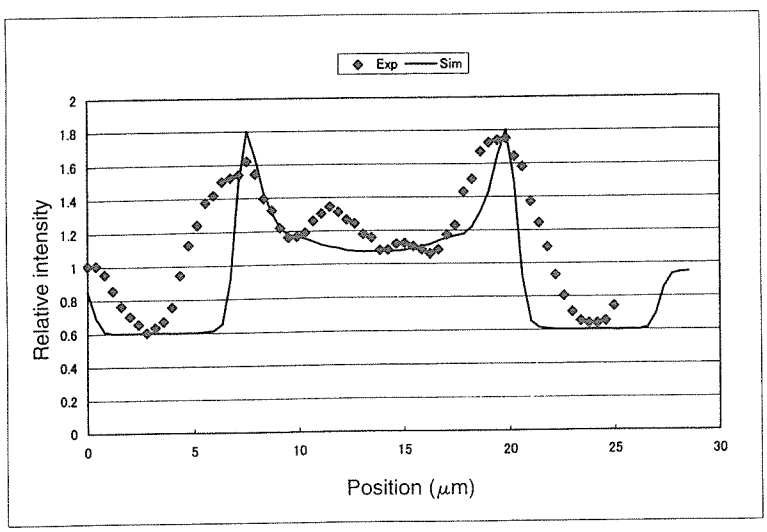

c | a / b

Fig. 5. a: Experimental image of Haversian canal.
b: Simulated image.
c: Profile curves of experimental and simulated images.

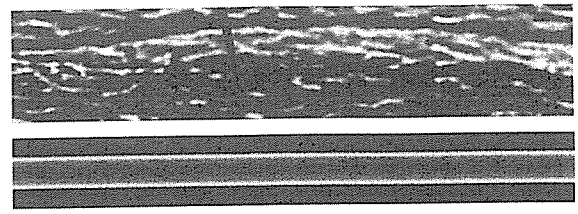

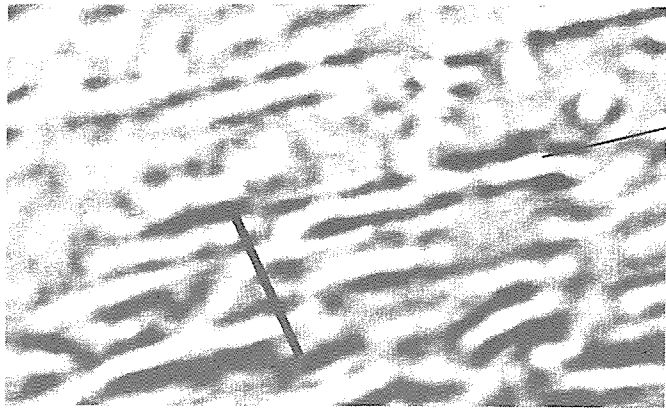

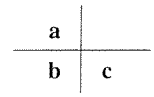

Fig. 6. a: Magnified images of canaliculus, small blood vessel, osteocytes, and trabecula.
b: Profile curve along line in Fig. 6a.
c: Auto-correlation function of profile curve in Fig. 6b.

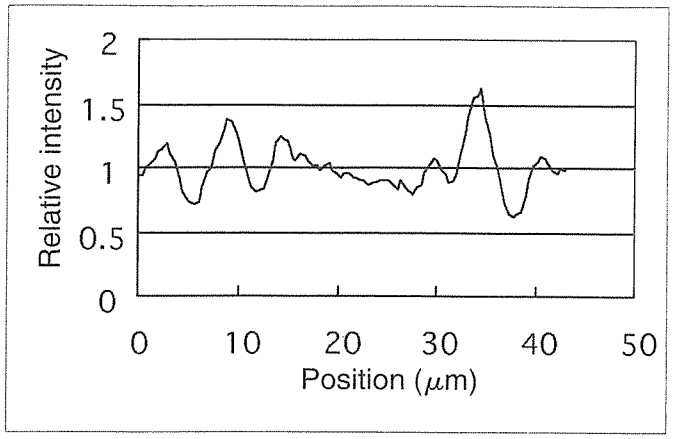

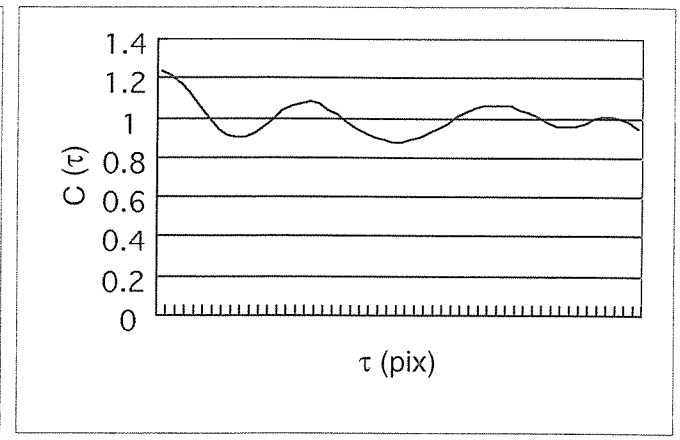

by preparing samples. There is minimal sample destruction in X-ray microscopic imaging, and the potential exists to observe the fine structure of thin living bone tissue using high coherence X-rays.

Acknowledgments

The authors would like to thank Dr. Masami Ando and Dr. Yoshiki Kohmura for helpful discussions. This study was partly funded by a research grant (No. 14570899) from the Ministry of Education, Culture, Sports, Science and Technology.

References

1) Snigirev A, Snigireva I, Kohn V, Kuznetsov S, Schelokov I. On the possibilities of x-ray phase contrast microimaging by coherent high-energy synchrotron radiation. *Rev Sci Instrum,* 66: 5486–5492, 1995.
2) Hirano M, Yamasaki K, Nagai H, *et al.* Radiation dose and spatial resolution evaluation in SR imaging. In *Proc. Workshop on Medical Applications of Synchrotron Radiation,* ESRF, p. 54, 2001.
3) Hirano M, Yamasaki K, Nagai H, *et al.* Refraction-enhanced X-ray imaging of 10 m distance using synchrotron radiation source. In *Proc. of Joint Symposium on Bio-Sensing and Bio-Imaging,* 1B-8: pp. 128–129, 2001.
4) Alfelli F, Bonvicini V, Bravin A, *et al.* Mammography with synchrotron radiation: phase-detection techniques. *Radiology,* 215: 286–293, 2000.
5) Yagi N, Suzuki Y, Umetani K, *et al.* Refraction-enhanced x-ray imaging of mouse lung using synchrotron radiation source. *Med Phys,* 26: 2190–2193, 1999.
6) Kono M, Obayashi C, Yamasaki K, *et al.* Refraction imaging and histologic correlation in excised tissue from a normal human lung. *Acad Radiol,* 8: 898–902, 2001.
7) Momose A, Takeda T, Itai Y, Yoneyama A, Hirano K. Perspective for medical applications of phase-contrast X-ray imaging. In *Medical Applications of Synchrotron Radiation,* (Ando M, Uyama C eds.; Springer-Verlag, Tokyo), pp. 54–62, 1998.
8) Takano H, Suzuki Y, Uesugi K, Takeuchi A, Yagi N. Point spread function measurement of imaging detectors with an x-ray microbeam. In *Proc. of the SPIE Conference,* 4499: p.126, 2001.
9) Mori K, Sekine N, Sato H, *et al.* Development of phase contrast radiography for bone imaging using synchrotron radiation. *Anal Sci,* 17: i1427–1430, 2001.
10) Harris J. Histology: the lives and death of cells in tissues. In *Molecular Biology of the Cell, 4th ed.* (Alberts B, Bray D eds.; Garland Science, NY), p. 1306, 2002.

Available online at www.sciencedirect.com
SCIENCE DIRECT®
Neuroscience Research 50 (2004) 467–474
Neuroscience Research
www.elsevier.com/locate/neures

Glycolysis regulates the induction of lactate utilization for synaptic potentials after hypoxia in the granule cell of guinea pig hippocampus

Toshihiro Takata[a,*], Bo Yang[a], Takashi Sakurai[a], Yasuhiro Okada[b], Koichi Yokono[a]

[a]*Department of Internal and Geriatric Medicine, Kobe University Graduate School of Medicine, 7-5-1 Kusunoki-cho, Chuo-ku, Kobe 650-0017, Japan*
[b]*Health Sciences Center, Kobe Health-Life Plaza, 5-1-2-300, Hyogo-ku, Kobe, Japan*

Received 9 June 2004; accepted 19 August 2004
Available online 21 September 2004

Abstract

Lactate is considered an alternative substrate that is capable of replacing glucose in maintaining synaptic function in adult neurons. But, we found recently that lactate could be utilized for maintenance of synaptic potentials only after the activation of NMDA and voltage-dependent-calcium channel during glucose deprivation. To clarify more on the relationship between glycolysis and induction of lactate utilization, we tested lower concentration of glucose with hypoxia to induce a relative shortage of anaerobic energy production. Population spikes are not maintained with lactate following hypoxia in 10 mM glucose medium, but are maintained at their original levels with lactate after exposure to hypoxia in lower concentration (5 mM) of glucose. Hypothermia during low glucose-hypoxia, bath application of the NMDA channel blocker and the voltage-sensitive calcium channel blocker, as well as the omission of extracellular calcium prevented the induction of the lactate-supported population spikes. ATP levels in the tissue slices are relatively preserved in the conditions that block the induction of lactate-supported population spikes. From these observations, we propose that the energy source for maintenance of synaptic function in adult neuron changes from adult form (glucose alone) to immature one (glucose and/or lactate) after short of glucose supply.
© 2004 Published by Elsevier Ireland Ltd and the Japan Neuroscience Society.

Keywords: Glycolysis; Lactate; Field potential; NMDA receptor; Voltage-sensitive calcium channel; Adenosine triphosphate; Glutamate release

1. Introduction

It is well known that lactate can be utilized as an energy substrate instead of glucose in the immature brain (Wada et al., 1997) and that it can also be used to maintain the energy level of the mature brain (Saitoh et al., 1994; Kanatani et al., 1995; Wada et al., 1998). Under ordinary conditions, glucose is the primary substrate in the brain for the maintenance of basic synaptic activity (Cox and Bachelard, 1988; Takata and Okada, 1995; Dienel and Hertz, 2001) and for providing energy to maintain the activated state (Fox et al., 1988; Roberts, 1993; Chih et al., 2001a,b). However, the role of lactate in the maintenance of synaptic function in the adult brain is controversial (Schurr, 1988; Fowler, 1993; Takata and Okada, 1995; Izumi et al., 1997; Takata et al., 2001; Dienel and Hertz, 2001). In rapidly prepared hippocampal slices (which are supposed to yield less damaged neurons; Yamane et al., 2000), synaptic potentials cannot be preserved in circulating medium containing lactate instead of glucose (Saitoh et al., 1994; Takata and Okada, 1995; Yamane et al., 2000; Takata et al., 2001). Synaptic potentials can, however, be well-maintained in lactate medium after the slices have undergone glucose deprivation or if the hippocampus slices are prepared slowly under condition thought to mimic ischemia (Sakurai et al., 2000; Yamane et al., 2000). In addition, synaptic potentials recorded at reduced temperature (e.g., 30 °C; Izumi et al., 1997, 29 °C; Takata et al., 1997) show dramatic resistance to glucose deprivation, suggesting that mild hypothermia itself covers the significant role of anaerobic glycolysis for maintenance of the synaptic potential at higher physiological temperature (Takata et al., 1997). Therefore, the results of the experiments conducted at reduced temperature require careful interpretation, especially when they are related to metabolic processes such as glycolysis. These results

* Corresponding author. Tel.: +81 78 382 5901; fax: +81 78 382 5919.
E-mail address: takata-tky@umin.ac.jp (T. Takata).

0168-0102/$ – see front matter © 2004 Published by Elsevier Ireland Ltd and the Japan Neuroscience Society.
doi:10.1016/j.neures.2004.08.008

suggest that lactate can support synaptic potentials under conditions similar to post-insult states or in a protective environment such as hypothermia.

We have demonstrated that the population spikes (PS) in the dentate gyrus (DG) of the hippocampus spontaneously recover after transient suppression during lactate replacement for glucose (Saitoh et al., 1994; Takata et al., 2001). This phenomenon is dependent upon activation of *N*-methyl-D-aspartate (NMDA) receptors and voltage-sensitive calcium channels (VSCCs; Takata et al., 2001). We have proposed that lactate will only be efficiently utilized for the maintenance of synaptic potentials after a trigger event that induces Ca^{2+} influx, such as hypoglycemia or other cytotoxic insults (Takata et al., 2001). With regard to energy metabolism in the neuron, we hypothesize that synaptic function is maintained by both anaerobic glycolysis and mitochondrial oxidation, and that anaerobic glycolysis plays an essential role in the maintenance of synaptic potentials in spite of its minor contribution towards energy production (Takata and Okada, 1995; Yamane et al., 2000; Takata et al., 2001). Furthermore, energy utilization for synaptic function may be regulated via a mechanism which involves switching from anaerobic to aerobic glycolysis in response to Ca^{2+} influx. To better understand the switching mechanism enabling the use of lactate for maintaining synaptic potentials, we analyzed the effect of hypoxia on lactate utilization for maintenance of PS under conditions of varying glucose concentrations. Under these conditions, enhanced glycolysis (a Pasteur effect) induced by hypoxia highlights the role of anaerobic glycolysis for the induction of lactate utilization to maintain synaptic potentials. The introduction of hypothermia during hypoxia was employed to examine the utilization of lactate for synaptic potential maintenance under conditions in which glucose consumption is relatively spared. In conjunction with the electrophysiological study, we also examined the levels of ATP and extracellular glutamate in the hippocampal slices during hypoxia under varying glucose conditions.

2. Materials and methods

2.1. Preparation of hippocampal slices

Adult guinea pigs (Hartley, SLC, Japan), weighing 200–300 g, were sacrificed according to the guidelines for animal experimentation at the Kobe University School of Medicine. Hippocampus slices (300–400 μm) were prepared by cutting transversely along the long axis of the hippocampus as described (Okada, 1988). Each slice was preincubated for 20 min in the standard medium (in mM: NaCl 125, KCl 4, KH_2PO_4 1.24, $MgSO_4$ 1.3, $CaCl_2$ 2, $NaHCO_3$ 26, glucose 10) bubbled with 95% O_2 and 5% CO_2 at 35 °C and was kept at room temperature until usage. For the experiment of reduced level of glucose during hypoxia, we chose 5 mM because it is the critical level that the population spikes can be recorded stably from hippocampal slice (Li et al., 2000).

2.2. Electrical activity recording

After preincubation, each slice was transferred to an observation chamber equipped with a stereoscope. The chamber was perfused continuously with the standard medium at a flow rate of 4 ml/min. With this perfusion speed, the medium in recording chamber is replaced in 3 min. The temperature was maintained at 35 °C throughout the experiment with an incubator and temperature controller (PDMI-2, Medical Systems Corp., NY). The temperature of the incubator was continuously monitored and with this system, hypothermia from 35 to 30 °C can be achieved within 3 min. As an index of neural activity, the perforant path was stimulated at 0.1 Hz with constant current pulses (0.1 ms) and population spikes (PS) were recorded from the granule cell layer of the dentate gyrus (DG) with glass microelectrodes filled with 2 M NaCl. The stimulation intensity was adjusted to obtain PS amplitudes at 60–70% of the maximum elicited by supramaximal stimulation. After recording steady potentials for at least 20 min, the slices were perfused with conditioned medium. Hypoxia was introduced by switching to the perfusion medium bubbled with 95% N_2/5% CO_2. To test the effects of lactate during deprivation of glucose, glucose in the medium was replaced with 10 mM sodium lactate (lactate medium). Adding sodium lactate did not influence the pH of the medium.

2.3. ATP determination

DG regions were dissected from hippocampal slices under a stereoscope. After preincubation for 20 min in oxygenated standard medium at 35 °C, the dissected slices were incubated for 10 min in either standard medium (10 mM glucose), 5 mM glucose medium or hypoxic glucose-free medium bubbled with 95% N_2/5% CO_2. At the end of the incubation, the DG regions of four slices were immediately homogenized in 0.5 N perchloric acid with 1 mM ethylenediaminetetraacetic acid (EDTA) and centrifuged for 15 min at 2000 rpm. The supernatant was neutralized with 2 M $KHCO_3$, recentrifuged and stored at −30 °C until assay of ATP. ATP was quantitated enzymatically and fluorometrically by measuring the production of nicotinamide adenine dinucleotide phosphate hydride (NADPH; Okada, 1974). Protein content of the slices was determined by the method of Lowry and Passonneau (1951).

2.4. Determination of glutamate release

After preincubation (see above), 4–5 DG slices were incubated for another 20 min in 300 μl of standard medium bubbled with 95% O_2/5% CO_2 at 35 °C and the basal level of glutamate in the medium was determined. Hypoxia experiments were performed using medium bubbled with

95% N_2/5% CO_2. The concentration of glucose in the medium was either 0, 5, or 10 mM. After incubation in each medium, the quantity of glutamate released from the slices was determined by high performance liquid chromatography (HPLC). Prior to chromatography, the medium was filtered through 0.22 μm Millipore filters. Aliquoted medium (6 μl) was injected into vials and placed in a refrigerated automicrosampler (CMA/200, CMA, Stockholm). Samples were mixed with reagents, applied to a reverse-phase column (BAS, Tokyo), and the column eluate was monitored with a fluorescence detector (CMA/280, CMA, Stockholm). Analyzed data were printed out with a chromatographic recorder (D-2500, Hitachi, Tokyo). Sample concentrations were calculated using chromatograms generated with known concentrations of amino acid standards.

2.5. Materials

ATP, protein assay reagents, nimodipine and D-(-)-2-amino-5-phosphonovaleric acid (APV) were purchased from Nacalai Co., Japan. Hexokinase, glucose-6-phosphatedehydrogenase (G6PDH) and all other enzymes were obtained from Boehringer Mannheim, Germany. Sodium lactate was obtained from Sigma, U.S.A.

2.6. Statistical analysis

Values are shown as mean ± S.E.M. Statistical analysis was performed by ANOVA and Bonferroni post hoc test and paired *t*-test. Treatment differences were considered significant at $P < 0.05$.

3. Results

3.1. The induction of lactate-supported PS is dependent on glucose and the activation of NMDA/VSCC

The time course of PS during hypoxia for 10 min and subsequent replacement of glucose with lactate is shown in Fig. 1. The amplitude of PS rapidly declines in a similar manner during hypoxia in medium containing 5 or 10 mM glucose. Surprisingly, the PS amplitude is maintained after replacement of lactate for glucose when the glucose content during hypoxia exposure is 5 mM while it is transiently reduced and subsequently recovers in the 10 mM glucose medium (Fig. 1).

We previously demonstrated that the transient block and subsequent recovery of synaptic potentials in the DG of the hippocampus after replacement of lactate for glucose is dependent on the activation of NMDA receptors and VSCCs (Takata et al., 2001). Thus, we next studied the effect of the NMDA receptor antagonist, APV, and the VSCC antagonist, nimodipine, on the induction of lactate-supported PS after exposure to low glucose and hypoxia. During hypoxia with 5 mM glucose medium, 50 μM both APV and nimodipine

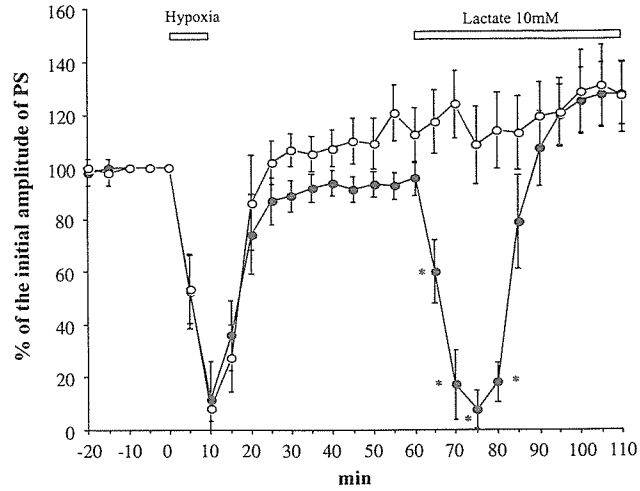

Fig. 1. Time course of the change in the amplitude of population spikes after exposure to hypoxia using 5 mM (open circles) or 10 mM glucose (filled circles) in the perfusion medium. Hypoxia was introduced for 10 min and glucose was replaced with 10 mM lactate in the perfusion medium after recovery from hypoxia exposure as indicated by the open horizontal bars. The ordinate is the percent of the initial amplitude of population spikes recorded from the granule cell layer of hippocampal dentate gyrus. Each plot indicates the mean value ± S.E.M. of five slices. Asterisks indicate a significant difference in amplitude between 5 and 10 mM glucose conditions.

were applied to the perfusion medium. Under these conditions, the PS amplitude is not maintained following lactate substitution and shows a transient block with subsequent recovery similar to that observed with the medium containing 10 mM glucose in the original experiment (Fig. 2). This result suggests that the induction of lactate-supported PS after hypoxia with the lower glucose level is also dependent on the activation of NMDA receptors

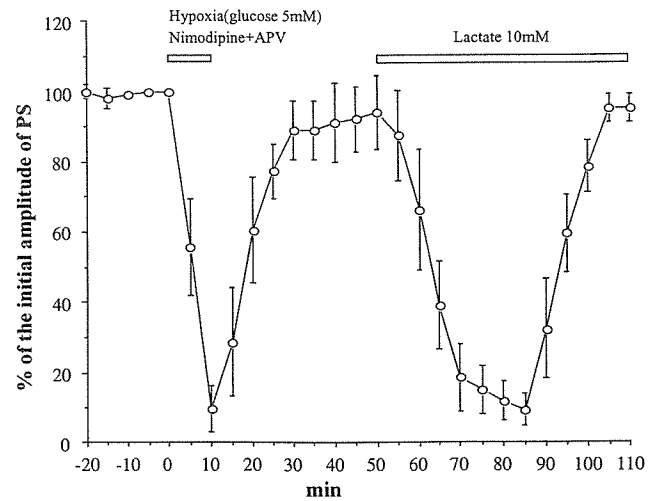

Fig. 2. Effect of APV and nimodipine on the change in amplitude of population spikes during subsequent replacement of glucose with lactate. The NMDA receptor antagonist, APV, and voltage-sensitive calcium channel antagonist, nimodipine, were included in the perfusion medium containing 5 mM glucose during hypoxia as indicated by the horizontal bars. The ordinate is the same as in Fig. 1. Each plot indicates the mean value ± S.E.M. of five slices.

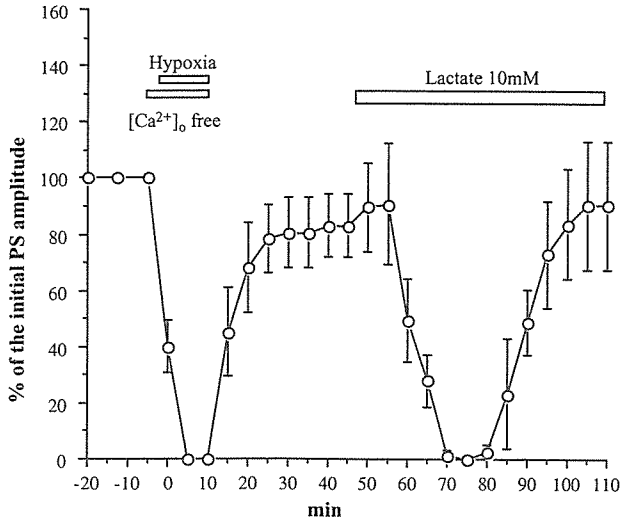

Fig. 3. Effect of the omission of extracellular calcium during hypoxia on the amplitude of population spikes during subsequent replacement of glucose with lactate. Calcium was omitted from the perfusion medium containing 5 mM glucose and 200 μM EGTA was added (to remove any free Ca^{2+}) 5 min before start of hypoxia as indicated by open horizontal bars. Zero minute on the horizontal axis indicates the start time of hypoxia. After recovery of PS amplitude, the perfusion medium was replaced with glucose-free medium containing 10 mM lactate as shown. The ordinate is the same as in Fig. 1. Each plot indicates the mean value ±S.E.M. of five slices.

and VSCCs. We did not observe the same phenomenon after ischemia-like conditions (hypoxia and glucose-free medium); recovery from such a severe challenge is rare (data not shown).

To further elucidate the role of Ca^{2+} influx through the NMDA receptor and VSCCs, slices were subjected to hypoxia with 5 mM glucose, but no Ca^{2+} in the perfusion medium (Fig. 3). The time course of the PS amplitude exhibits a transient block of PS with recovery during lactate replacement for glucose, indicating that the effect of the low glucose level seen in Fig. 1 is negated without extracellular calcium. The level of 5 mM glucose itself is sufficient for maintenance of PS in the dentate gyrus of hippocampus (Kanatani et al., 1995; Li et al., 2000). These results demonstrate that the induction of lactate-supported PS is dependent on Ca^{2+} influx through the NMDA receptor and the VSCC, and that the small reduction of glucose levels (from 10 to 5 mM), which does not influence the basic PS amplitude, triggers the activation of these channels during hypoxia.

3.2. *Hypothermia can prevent the induction of lactate utilization for PS*

Mild hypothermia (33–29 °C) drastically reduces Ca^{2+} accumulation in the cell and improves the recovery of PS after oxygen and/or glucose deprivation (Takata et al., 1997). Furthermore, we previously reported that hypothermia prevented the decline of PS and ATP levels in the slices, particularly during glucose deprivation. These results suggest that a component of the mechanism used to sustain PS and ATP levels by anaerobic glycolysis is highly temperature sensitive (Takata et al., 1997). Based on these observations, we proposed that hypothermia will prevent the reduction of ATP levels that may trigger the activation of the NMDA receptor and the VSCC. First, we tested the effect of hypothermia on PS amplitude in lactate medium at 30 °C. Upon lowering the temperature to 30 °C with 10 mM glucose, an initial mild transient depression (80% of the initial amplitude) of PS is observed, after which the amplitude rises to 120% (Fig. 4A). The temperature of 30 °C was chosen because a previous report by Aihara et al. (2001) showed that, within the range of 17–36 °C, 30 °C resulted in PS with the highest amplitude. Indeed, the degree of increase of PS in our experiments is almost identical with their results. By selecting the temperature at which the amplitude of PS is maximized, we can see easily the response in PS when there is a depressive effect from energy deprivation. Next, lactate was introduced and the amplitude of PS initially increased to 140% and subsequently stabilized at 120–130% (Fig. 4A). This result confirms that lactate can maintain synaptic potentials at 30 °C for at least 60 min as in the case of glucose deprivation with hypothermia. When hypothermia is introduced during hypoxia with 5 mM glucose in the perfusion medium, the PS amplitude is reduced to 60% and recovers fully after recirculation of standard oxygenated medium at 35 °C. After replacement of glucose with lactate, a transient blockade and subsequent spontaneous recovery of PS results (Fig. 4B). This suggests that hypothermia prevents the exhaustion of energy originating from anaerobic glycolysis and maintains the essential energy levels that prohibit the induction of lactate-supported synaptic potentials.

3.3. *ATP levels in the DG region*

Lowering the glucose levels in the medium during hypoxia enables PS to be maintained at the original levels in the lactate medium, however, hypothermia prevents this maintenance effect. We next determined the energy (i.e., ATP) levels in the slices under both conditions. The DG region of each slice was selectively dissected and incubated for 10 min in standard medium (containing 10 mM glucose), glucose-free medium (ischemia-like conditions), or 5 mM glucose medium bubbled with 95% N_2/5% CO_2 (hypoxic conditions). The ATP concentration of each sample was determined by a sensitive microassay method (Okada, 1974). ATP levels in the slices are 13.6 ± 0.55 mmol/kg protein under the control conditions (10 mM glucose bubbled with 95% O_2/5% CO_2). ATP levels were reduced in each experimental case relative to the control. The ATP level was 12.8% of the control level under ischemia-like conditions, 36% of the control in 5 mM glucose medium with hypoxia, and 66.6% of the control in 10 mM glucose medium with hypoxia (Fig. 5). When hypothermia is introduced with the 5 mM glucose-containing medium, the

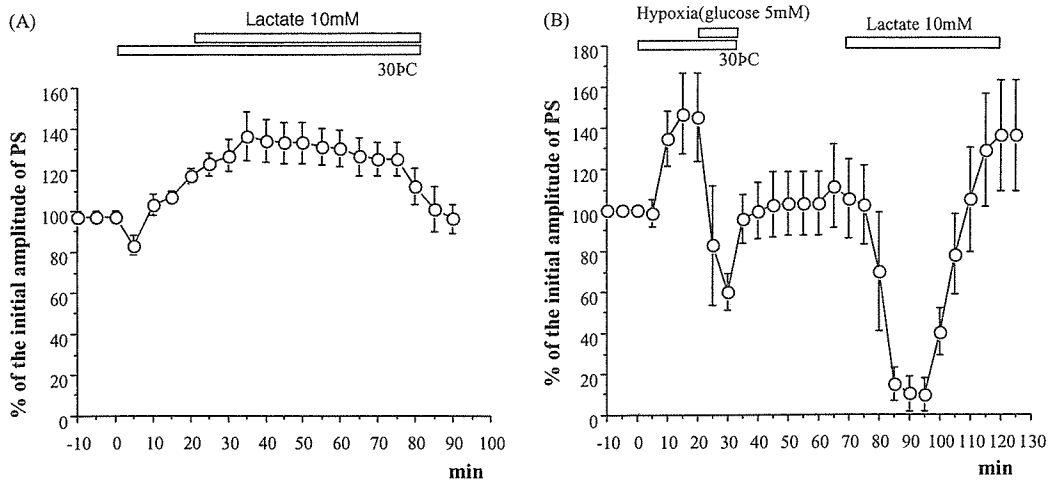

Fig. 4. (A) Effect of hypothermia on the amplitude of population spikes over time. Hypothermia at 30 °C was introduced and 10 mM glucose in the perfusion medium was replaced with lactate as indicated by the open horizontal bars. (B) Effect of hypoxia with 5 mM glucose combined with hypothermia on the amplitude of population spikes after replacement of glucose with lactate. Hypothermia at 30 °C was introduced prior to hypoxia with 5 mM glucose. After recovery from hypoxia, glucose was replaced with lactate as indicated by the open horizontal bars. The ordinate is the same as in Fig. 1. The last half of control data (10 min out of 20 min observation) is shown in both (A) and (B). Each plot indicates the mean value ± S.E.M. of five slices.

ATP levels are significantly preserved at 64.9% of the control levels ($P < 0.001$; Fig. 5). These results indicate that hypothermia preserves the energy levels in the slices during hypoxia and that the energy levels measured in the slices during hypoxia correlate with the subsequent induction of lactate-supported synaptic potentials.

3.4. Glutamate release from the DG region

Energy deprivation, such as hypoxia or hypoglycemia, induces extracellular glutamate accumulation (Choi, 1988; Katayama et al., 1991; Takata et al., 1995). We previously demonstrated that extracellular glutamate levels increased when lactate was substituted for glucose (Takata et al., 2001). To investigate the correlation between extracellular glutamate levels and the induction of lactate utilization after hypoxia with low glucose in the medium, the glutamate levels in the medium under different conditions were determined using HPLC. The basal level of glutamate released in the medium is 1.17 ± 0.075 μM/mg protein. After 10 min of incubation under ischemia-like conditions, the released levels of glutamate modestly increase and prominently increase after 30 min. The glutamate levels in the medium with 5 mM glucose do not increase even after 30 min exposure to hypoxia (data not shown).

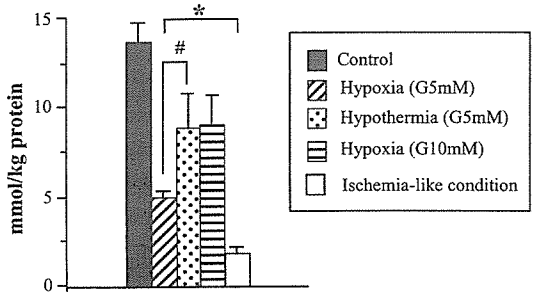

Fig. 5. Concentration of ATP from dentate gyrus of hippocampus during hypoxia with 5 mM glucose (G5mM), 10 mM glucose (G10mM), G5 mM + hypothermia, and ischemia-like conditions (hypoxia + glucose-free). The ordinate is the average ATP concentration (in mmol ATP/kg protein) ± S.E.M. from four dissected parts of dentate gyri from hippocampus. *Significantly different when compared with the control. #Significant difference between the 5 mM glucose and 5 mM glucose + hypothermia groups.

4. Discussion

Saitoh et al. (1994) found that the PS amplitude measured from the granule cell of dentate gyrus from the guinea pig hippocampus spontaneously recovered after a transient blockade when glucose in the perfusion medium was substituted with lactate. Kanatani et al. (1995) confirmed that glucose metabolites such as fructose, pyruvate and lactate preserved ATP and creatine phosphate levels in the slices although the PS amplitude was not maintained. We investigated further using intracellular recording techniques and reported that the spontaneous recovery of synaptic potentials following lactate substitution for glucose was not observed in CA3 pyramidal neurons and that lactate could not support synaptic potentials (Takata and Okada, 1995). Early studies proposed that the decline of ATP levels is responsible for the suppression of the synaptic potentials during energy deprivation (Lipton and Whittingham, 1982; Martin et al., 1994). However, the fact that synaptic potentials cannot be supported despite the maintenance of energy levels suggests that reduced ATP is not the only explanation for the loss of synaptic potentials. We proposed that there are distinct roles for anaerobic and aerobic glycolysis and reported that there is a difference in the mechanism by which synaptic potentials are suppressed when the cells are deprived of glucose versus oxygen that

cannot be explained solely by energy metabolism (Takata and Okada, 1995). Furthermore, a switching mechanism between anaerobic and aerobic glycolysis that is dependent on the NMDA receptor and VSCCs (Takata et al., 2001) is suggested since lactate can support synaptic potentials after exposure to glucose deprivation (Sakurai et al., 2000; Takata et al., 2001). Yamane et al. (2000) demonstrated that damaged hippocampal slices containing low levels of ATP could use lactate for maintenance of PS. Summarizing these observations, the induction of lactate utilization for maintenance of synaptic potentials is triggered by conditions of limited glucose such that the energy source dependency may change from glucose alone (adult form) to utilization of glucose and/or lactate that may be called, immature form.

4.1. Effect of lowering glucose levels during hypoxia on induction of lactate-supported PS

When lowering glucose levels to 5 mM in the perfusion medium, exposure of the hippocampal slice to hypoxia induces the utilization of lactate for the maintenance of PS. This is in contrast with the result from the medium containing 10 mM glucose, in which lactate cannot support the PS amplitude (Fig. 1). The effect of lower glucose levels is abolished by applying antagonists of the NMDA receptor and the VSCC (Fig. 2) in the perfusion medium, omission of Ca^{2+} from the perfusion medium (Fig. 3), or introduction of hypothermia during hypoxia (Fig. 4B). Because the antagonists of the NMDA receptor and the VSCC block the induction of lactate-supported potentials following hypoxia, we propose that the activation of these channels is necessary for the induction of lactate usage for maintenance of PS as in the case of glucose deprivation (Takata et al., 2001). Furthermore, the failure of lactate to maintain PS after hypoxia exposure in calcium-free medium supports the involvement of these channels.

4.2. Hypothermia also blocks the induction of lactate usage for PS maintenance

We further examined the effect of hypothermia on the induction of lactate utilization to support potentials. Hypothermia reduces ischemic brain damage (Busto et al., 1987), and a small reduction in the temperature significantly improves the recovery of field potentials and retains the energy levels of hippocampal slices during oxygen and/or glucose deprivation (Takata et al., 1997). Furthermore, reducing the temperature from 35 to 30 °C reduces the rate of energy usage in these slices by about 30% (Okada, 1988). To simulate the conditions of energy conservation during hypoxia, the temperature of the incubator containing 5 mM glucose medium was reduced to 30 °C (Fig. 4B). Hypoxia increases the basal level of the PS amplitude (Aihara et al., 2001), reduces the PS decline during hypoxia and prevents the induction of lactate usage for PS maintenance (Fig. 4B). This indicates that the mechanism used to preserve energy prevents the induction of lactate usage for PS maintenance.

4.3. ATP levels in the dentate gyrus during hypoxia with low glucose

Hypoxia induces an accelerated rate of glycolysis to compensate for the lack of energy production from the TCA cycle (a Pasteur effect). Although it also results the decline of ATP levels of hippocampal slices (Fig. 5), the PS amplitude shows full recovery after reintroduction of the standard medium. Under ischemia-like conditions when the ATP level falls to approximately 2 mmol/kg protein (Fig. 5), the PS cannot be evoked again following recirculation of normal oxygenated medium after up to 60 min (data not shown). There may be a critical ATP level in the range of 2–5 mmol/kg protein in our experimental setting after which the PS does not recover. Wang et al. (2000) reported that an ATP level of approximately 1 nmol/mg dry weight protein (note: wet weight protein is used in our report) determines the reversibility of synaptic potentials in the CA1 pyramidal neurons. In comparing the original ATP levels reported by Wang et al. (2000) (6.1 nmol/mg protein) to our original ATP levels (13.6 mmol/kg protein) the levels that determine synaptic potential irreversibility may be similar (16% versus 15% of the original levels). We have found that the ATP level is significant not only for determining whether synaptic function can be recovered, but it is also correlated with the energy source dependency (adult or immature form) at higher levels (5 mmol ATP/kg protein or 37% of the initial levels) under these experimental conditions. The ATP levels are identical in experiments using 5 mM glucose + hypothermia to those using medium containing 10 mM glucose under hypoxia (Fig. 5). This also explains the inverse correlation of ATP levels and the induction of lactate-supported PS.

4.4. Extracellular glutamate concentration during hypoxia

We reported previously that a blockade of synaptic potential during hypoxia alone was not accompanied with a robust increase of intracellular calcium ($[Ca^{2+}]_i$), as in the case of glucose deprivation or combined oxygen + glucose deprivation (Takata and Okada, 1995). Compared with combined oxygen + glucose deprivation, a hippocampal slice exposed to hypoxia alone has the potential to recover synaptic potentials in the presence of a sufficient supply of glucose (Tian and Baker, 2000). The moderate decrease in ATP levels compared with that seen under ischemia-like conditions (Fig. 5) prevents the reverse action of the glutamate transporter or blocks the glial glutamate transporter (Erecinska and Dagani, 1990). It is surprising that NMDA and VSCC antagonists prevent the induction of lactate-supported PS in the apparent absence of extracellular glutamate release during hypoxia under the conditions of